PCCP

PAPER

View Article Online
View Journal | View Issue

Cite this: *Phys. Chem. Chem. Phys.*, 2023, **25**, 11658

A new computational tool for interpreting the infrared spectra of molecular complexes†

Alex Iglesias-Reguant, [ab] Heribert Reis,[c] Miroslav Medveď, [de] Josep M. Luis *[b] and Robert Zaleśny *[f]

The popularity of infrared (IR) spectroscopy is due to its high interpretive power. This study presents a new computational tool for analyzing the IR spectra of molecular complexes in terms of intermolecular interaction energy components. In particular, the proposed scheme enables associating the changes in the IR spectra occurring upon complex formation with individual types of intermolecular interactions (electrostatic, exchange, induction, and dispersion), thus providing a completely new insight into the relations between the spectral features and the nature of interactions in molecular complexes. To demonstrate its interpretive power, we analyze, for selected vibrational modes, which interaction types rule the IR intensity changes upon the formation of two different types of complexes, namely π···π stacked (benzene···1,3,5-trifluorobenzene) and hydrogen-bonded (HCN···HNC) systems. The exemplary applications of the new scheme to these two molecular complexes revealed that the interplay of interaction energy components governing their stability might be very different from that behind the IR intensity changes. For example, in the case of the dispersion-bound π···π-type complex, dispersion contributions to the interaction induced IR intensity of the selected modes are notably smaller than their first-order (electrostatic and exchange) counterparts.

Received 3rd August 2022,
Accepted 17th March 2023

DOI: 10.1039/d2cp03562f

rsc.li/pccp

1. Introduction

Intermolecular interactions are central to many areas of chemistry. Over the past several decades significant research effort has been made to understand the fundamental aspects of the interactions in molecular complexes and their manifestation, thus leading to stunning applications affecting practically all domains of everyday life including new opportunities in biomedical engineering, crystal engineering,[1] and transmembrane anion transport.[2] Spectroscopic techniques were frequently used to substantiate the formation and quantify the magnitude of intermolecular forces, with infrared (IR) spectroscopy at the forefront. One of the many examples is hydrogen-bonding interactions studied using IR spectroscopy as they are manifested by significant frequency shifts of the order of magnitude of hundreds of cm^{-1} and IR intensity changes of bands associated with the vibrational modes of functional groups involved in the hydrogen-bonding interactions.[3,4] The experimental efforts have been supported by theoretical developments within the quantum mechanics framework, and nowadays the theory of intermolecular interactions forms an important part of modern interpretive chemistry. Despite some variations among available intermolecular interaction energy decomposition schemes, the fundamental interaction types include electrostatics, Pauli exchange, induction and dispersion. These interaction types, and their various cross-terms, can be rigorously calculated using *e.g.* Symmetry-Adapted Perturbation Theory (SAPT).[5] There are also alternative strategies to decompose intermolecular interaction energies, often referred to as Energy Decomposition Analysis (EDA) approaches.[6–13] Some of them introduce electrostatic, Pauli, and orbital interaction terms, as in Ziegler–Rauk EDA (ZR-EDA),[7] or the mixture of both, that is, electrostatic, polarization, charge transfer, Pauli, and dispersion terms, as in the Absolutely Localized Molecular Orbital EDA (ALMO-EDA) methods.[14] The results of intermolecular interaction energy decompositions are available for myriads of atomic and molecular complexes, thus enriching our understanding of how the basic interaction types govern the structure and stability of molecular complexes and

[a] *Faculty of Chemistry, Nicolaus Copernicus University, Gagarina 7, PL-87100 Torun, Poland*
[b] *Institute of Computational Chemistry and Catalysis and Department of Chemistry, University of Girona, Campus de Montilivi, 17003 Girona, Catalonia, Spain. E-mail: josepm.luis@udg.edu*
[c] *Institute of Chemical Biology, National Hellenic Research Foundation (NHRF), Vassileos Constantinou Ave 48th, 116 35 Athens, Greece*
[d] *Department of Chemistry, Faculty of Natural Sciences, Matej Bel University, Tajovského 40, SK-97400 Banská Bystrica, Slovak Republic*
[e] *Regional Centre of Advanced Technologies and Materials, Czech Advanced Technology and Research Institute (CATRIN), Palacký University in Olomouc, Šlechtitelů 27, 783 71 Olomouc, Czech Republic*
[f] *Faculty of Chemistry, Wroclaw University of Science and Technology, Wybrzeże Wyspiańskiego 27, 50-370 Wrocław, Poland. E-mail: robert.zalesny@pwr.edu.pl*
† In memory of Professor Krzysztof Woliński.

their organization at the larger scale.[15,16] The spectroscopic measurements are often supported by the results of energy decomposition analyses, linking indirectly the spectroscopic signatures with interaction types. However, as we have learned from pioneering works of Fowler and Sadlej,[17] Bishop and Dupuis[18] and Heijmen, Moszyński *et al.*,[19] and their successors,[20–22] the pattern of interaction types may be very different for interaction energies (related to stability) and electric properties (relevant for intensities of spectral signatures). The latter quantities can be analyzed conveniently using the concept of *excess* (interaction-induced) properties (ΔP),[17,19–55] *i.e.*, for a complex **AB** composed of subsystems **A** and **B**:

$$\Delta P = P(\mathbf{AB}) - P(\mathbf{A}) - P(\mathbf{B}) \tag{1}$$

As highlighted above, the values of ΔP can be further analyzed in terms of fundamental interaction types ΔP^i.

The vast majority of works use eqn (1) to analyze the effect of intermolecular interactions on the pure electronic contribution to electric properties, $\Delta P^{\mathrm{el},i}$. In recent papers the authors introduced a new scheme for the decomposition of the excess vibrational nuclear relaxation contribution to electric properties.[56–58] The aim of the current work is to demonstrate how the recently developed decomposition scheme can be extended to gain an insight into the changes in the IR spectra upon complex formation in terms of interaction types, *i.e.*

$$\Delta I_a^i = I_a^i(\mathbf{AB}) - I_a^i(\mathbf{A}) - I_a^i(\mathbf{B}) \tag{2}$$

where, as previously, i denotes an interaction energy component and a stands for a normal mode of vibration. First, we will present a concise theoretical framework for the analysis of the excess IR intensities together with a decomposition scheme used to obtain individual interaction energy contributions. Then, the analysis of IR intensity changes for a few selected vibrational modes in benzene$\cdots$1,3,5-trifluorobenzene (B$\cdots$T) and HCN$\cdots$HNC complexes will be performed as a proof of concept.

2 Theory

The excess property decomposition scheme[56–58] relies on the electronic (ΔP^{el}) and nuclear-relaxation (ΔP^{nr}) contributions. The latter one usually provides the major vibrational contribution to the total response property change.[59] There is a link between the a-th mode contribution to the average nuclear-relaxation polarizability:[60–62]

$$\langle \alpha_a^{\mathrm{nr}} \rangle = \frac{1}{3} \sum_{j=x,y,z} \alpha_{jj,a}^{\mathrm{nr}} = \frac{1}{3\omega_a{}^2} \sum_{j=x,y,z} \left(\frac{\partial \mu_j}{\partial Q_a} \right)^2 \tag{3}$$

and the harmonic IR intensity for the a-th vibrational mode:

$$I_a = \frac{N\pi}{3c^2} \sum_{j=x,y,z} \left(\frac{\partial \mu_j}{\partial Q_a} \right)^2 \tag{4}$$

as both rely on the square of the first derivative of the dipole moment (μ) with respect to the normal mode Q_a. ω_a is the harmonic vibrational frequency of mode a, N is Avogadro's number, and c is the speed of light. Combining both equations leads to

$$\langle \alpha_a^{\mathrm{nr}} \rangle = \frac{c^2}{N\pi} \times \frac{I_a}{\omega_a{}^2} \tag{5}$$

The above relation can be used for interaction-induced counterparts:

$$\langle \Delta\alpha_a^{\mathrm{nr}} \rangle = \frac{c^2}{N\pi} \times \Delta\left(\frac{I_a}{\omega_a{}^2} \right) \tag{6}$$

In our previous work[58] we have demonstrated that the interaction-induced average nuclear-relaxation polarizability can be decomposed into interaction types i by employing the finite-field nuclear-relaxation (FF-NR) method:[63]

$$\langle \Delta\alpha^{\mathrm{nr},i} \rangle = -\frac{1}{3} \sum_{j=x,y,z} \frac{\partial^2 \left[\Delta E_{\mathrm{int}}^i(\mathbf{F}, \mathbf{AB}_F) - \Delta E_{\mathrm{int}}^i(\mathbf{F}, \mathbf{AB}) \right]}{\partial F_j^2} \tag{7}$$

where $\mathbf{AB}_F$ is the relaxed geometry of the complex **AB** in the presence of an electric field, F_j, whereas **AB** stands for the field-free equilibrium geometry of the complex. The field-dependent geometry optimizations required to determine $\mathbf{AB}_F$ should be performed strictly maintaining the Eckart conditions.[64,65] To obtain only the contribution of mode a to $\langle \Delta\alpha^{\mathrm{nr},i} \rangle$ (*i.e.* $\langle \Delta\alpha_a^{\mathrm{nr},i} \rangle$) the field-dependent geometry optimizations should be performed in the subspace defined by a single vibrational mode, a. Then, the relation between $\langle \Delta\alpha_a^{\mathrm{nr},i} \rangle$ and the shifts in the intensity and frequency of the mode a is given by

$$\langle \Delta\alpha_a^{\mathrm{nr},i} \rangle = \frac{c^2}{N\pi} \times \Delta\left(\frac{I_a^i}{\omega_a^{2,i}} \right) \tag{8}$$

This equation allows interpreting a simultaneous change in the IR intensity and the vibrational frequency upon the formation of a complex in terms of the interaction types, i:

$$\Delta\left(\frac{I_a^i}{\omega_a^{2,i}} \right) = \frac{I_a^i}{\omega_a^{2,i}}(\mathbf{AB}) - \frac{I_a^i}{\omega_a^{2,i}}(\mathbf{A}) - \frac{I_a^i}{\omega_a^{2,i}}(\mathbf{B}) \tag{9}$$

Eqn (9) can be used directly to decompose changes in the ratio of intensity and frequency squared for each mode upon complex formation, thus providing information regarding the interplay of interaction types and their manifestation through changes in band position and intensity. One can also consider two limiting cases of eqn (8): (a) constant transition intensity, or (b) constant transition frequency. The former is not of practical use as the relation $\Delta\omega_a^{2,i} \sim 1/\langle \Delta\alpha_a^{\mathrm{nr},i} \rangle$ does not allow for direct decomposition of frequency changes. However, if the frequency change for a target vibrational mode upon complex formation is negligible, then the above relation allows for the direct decomposition of the IR intensity change of the mode a:

$$\Delta I_a^i = \frac{N\pi\omega_a{}^2}{c^2} \times \langle \Delta\alpha_a^{\mathrm{nr},i} \rangle \tag{10}$$

and the total excess IR intensity is the sum of interaction types:

$$\Delta I_a = \sum_i \Delta I_a^i \tag{11}$$

In this work we will show how to benefit from the constant-frequency condition (limiting case (b)) which holds as a good

approximation, for all studied cases in this work. It should be noted that nuclear relaxation polarizability does not account for any anharmonic corrections; and likewise, the IR intensities are evaluated adopting the harmonic approximation.

3. Computational details

Eqn (7)–(10) can be combined with any energy decomposition analysis (SAPT, ZR-EDA, ALMO-EDA, *etc.*), provided that field-dependent interaction energy terms can be determined. In the present work we employ the decomposition of MP2 interaction energy based on the variational–perturbational decomposition scheme (VP-EDS),[66–69] in which the interpretation of the individual interactions is based on intermolecular perturbation theory.[70] In VP-EDS, the total interaction energy obtained in a supermolecular approach is partitioned into several interaction energy terms as defined in the symmetry-adapted perturbation theory (SAPT).[66–69] At the second-order Møller–Plesset perturbation theory level (MP2), the total VP-EDS interaction energy of the complex calculated by a supermolecular approach in the dimer-centered-basis set (DCBS)[71] is partitioned into the Hartree–Fock (HF) and the electron correlation interaction energy components:

$$\Delta E_{\mathrm{int}}^{\mathrm{MP2}} = \Delta E_{\mathrm{int}}^{\mathrm{HF}} + \Delta E_{\mathrm{corr}}^{\mathrm{MP2}} \tag{12}$$

The HF term can be further partitioned into the electrostatic interactions of the charge densities of the unperturbed subsystems, $\varepsilon_{\mathrm{el}}^{(10)}$, the exchange repulsion ($\Delta E_{\mathrm{ex}}^{\mathrm{HL}}$) and the charge delocalization ($\Delta E_{\mathrm{del}}^{\mathrm{HF}}$), which account for the exchange effects due to the Pauli antisymmetry principle and induction, respectively.

$$\Delta E_{\mathrm{int}}^{\mathrm{HF}} = \varepsilon_{\mathrm{el}}^{(10)} + \Delta E_{\mathrm{ex}}^{\mathrm{HL}} + \Delta E_{\mathrm{del}}^{\mathrm{HF}} \tag{13}$$

The second-order electron correlation term, $\Delta E_{\mathrm{corr}}^{\mathrm{MP2}}$:

$$\Delta E_{\mathrm{corr}}^{\mathrm{MP2}} = \varepsilon_{\mathrm{el,r}}^{(12)} + \varepsilon_{\mathrm{disp}}^{(20)} + \Delta E_{\mathrm{ex}}^{(2)} \tag{14}$$

includes the second-order dispersion interaction, $\varepsilon_{\mathrm{disp}}^{(20)}$, as well as the electron correlation correction to the first-order electrostatic interaction, $\varepsilon_{\mathrm{el,r}}^{(12)}$, and the remaining second-order electron correlation effects ($\Delta E_{\mathrm{ex}}^{(2)}$). The latter term accounts mainly for the uncorrelated exchange–dispersion and electron correlation corrections to the Hartree–Fock exchange repulsion.[68,70] The terms $\varepsilon_{\mathrm{el}}^{(10)}$ and $\varepsilon_{\mathrm{disp}}^{(20)}$ are obtained using standard polarization perturbation theory, whereas the term $\varepsilon_{\mathrm{el,r}}^{(12)}$ is calculated using the formula proposed by Moszyński *et al.*[72] The numbers n,m in the superscript of terms such as $\varepsilon_{\mathrm{el}}^{(nm)}$ refer to orders of perturbation in the intermolecular interaction operator (n) and intramonomer correlation operator (m), respectively.

Field-free equilibrium geometries of the two studied complexes were obtained by optimizations applying tight convergence criteria (10^{-11} Hartree and 10^{-9} Hartree Bohr^{-1} for energy and gradients, respectively) and employing the MP2 method in combination with the aug-cc-pVDZ (benzene$\cdots$1,3,5-trifluorobenzene) and aug-cc-pVTZ (HCN$\cdots$HNC) basis set.[73–75] The vibrational analysis was performed at the same level of theory to confirm that the optimized structures are minima. All field-free computations were performed using the Gaussian program.[76] Field-dependent geometry optimizations and property calculations were carried out using custom computer programs based on total energies obtained using the Gaussian program, enforcing again tight convergence thresholds. VP-EDS calculations of field-free and field-dependent interaction energy components were performed using a modified in-house version of the Gamess (US) program.[77,78]

4. Results and discussion

In order to demonstrate the interpretive power of the above described scheme we selected a benzene$\cdots$1,3,5-trifluorobenzene (B$\cdots$T) complex in stacked alignment and a hydrogen-bonded HCN$\cdots$HNC complex. There are several reasons behind the selection of these complexes: (a) $\pi\cdots\pi$ stacking and hydrogen-bonding interactions play a key role in the formation of organic complexes (both types of intermolecular interactions govern the stability of nucleic acids), (b) the prototypical stacked and hydrogen-bonded complexes can be reliably treated at the MP2 level of theory, (c) they are asymmetric, with one moiety acting as electron donor and the other as electron acceptor, and thus not only dispersion, but also other interaction types can be important, and (d) each complex is composed of two different subsystems, thus safeguarding an interesting vibrational structure, *i.e.* different types of normal modes are localized on interacting molecules.

We will start with the analysis of stacked B$\cdots$T complex. One normal mode of vibration localized on benzene (ν_{24}) and two (degenerate) localized on 1,3,5-trifluorobenzene (ν_{56}, ν_{57}) were selected. The simulated spectra and atomic displacements for the corresponding monomeric and dimeric vibrational normal modes are shown in Fig. 1. The dominant band of benzene corresponds to the C–H out-of-plane in-phase vibration (a_{2u}, top panel), while the most intense bands of 1,3,5-trifluorobenzene are given by two degenerate vibrations (1660.66 cm^{-1}) corresponding to symmetric and asymmetric C–C stretching (middle panel). The bottom panel shows the spectra of the benzene$\cdots$1,3,5-trifluorobenzene complex in stacked alignment (the equilibrium geometry is presented in the inset). All spectra were simulated assuming Lorentzian band broadening and half width at half maximum equal to 10 cm^{-1}. There are two reasons behind the selection of these modes. First, these modes contribute to the largest-intensity peaks in the IR spectra of monomers, *i.e.*, ν_6 (benzene), ν_{26} and ν_{27} (1,3,5-trifluorobenzene). Second, they exhibit significant IR intensity changes upon complex formation. As shown in Table 1, the intensity of the mode ν_{24} of B$\cdots$T complex, attributed to the in-phase out-of-plane bending of hydrogen atoms on benzene increases in comparison with the corresponding mode of isolated benzene, while the two other modes, corresponding to symmetric and asymmetric C–C stretching vibrations localized on 1,3,5-trifluorobenzene, respectively, exhibit a significant intensity drop upon B$\cdots$T complex formation. Note that for all three selected normal modes the vibrational frequency shift on passing from the

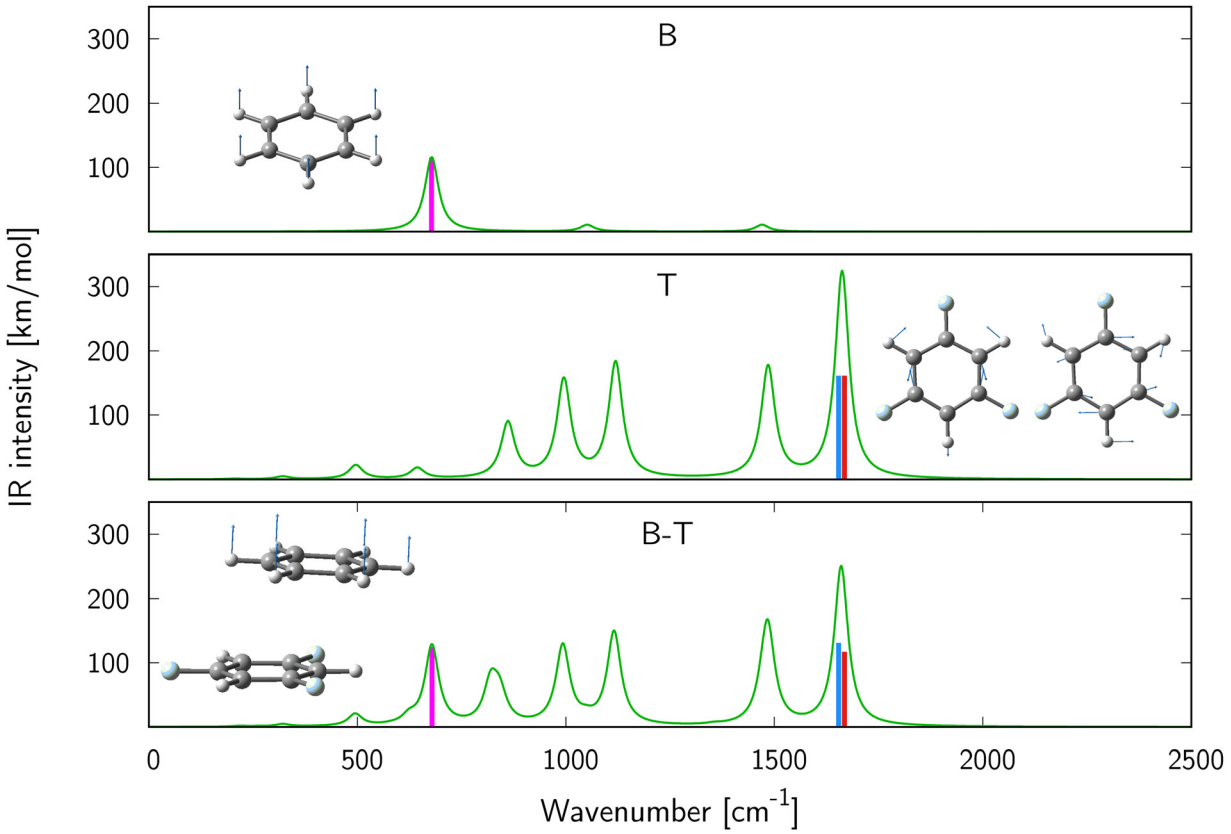

Fig. 1 Simulated IR spectra of benzene (top), 1,3,5-trifluorobenzene (middle) and their complex (bottom). Insets show atomic displacements corresponding to vibrational normal mode ν_6 of benzene (top), ν_{26} and ν_{27} (middle) mode of 1,3,5-trifluorobenzene, and ν_{24} (bottom) of the complex. Bands corresponding to C–H stretching (>3000 cm^{-1}) are not shown.

Table 1 Selected normal modes and their spectroscopic data. The values corresponding to complexes are shown in parentheses

	Mode	ω (cm^{-1})	I (km mol^{-1})	ΔI (km mol^{-1})
Benzene (B)···1,3,5-trifluorobenzene (T)				
B	ν_6 (ν_{24})	678.34 (678.85)	115.91 (124.63)	8.72
T	ν_{26} (ν_{56})	1662.66 (1660.25)	160.95 (130.95)	−30.00
T	ν_{27} (ν_{57})	1662.66 (1660.40)	160.95 (116.95)	−44.00
HCN···HNC				
—	— (ν3)	— (173.95)	— (5.97)	5.97
HCN	ν_4 (ν12)	3495.61 (3446.55)	77.28 (166.27)	88.99

isolated subsystems to the B···T complex is very small (not exceeding 3 cm^{-1}). Hence, one can safely employ eqn (10) to decompose the IR intensity changes (ΔI) induced by complex formation into individual interaction types (Table 2). The reported intermolecular interaction energy terms (ΔE_{int}) indicate, as expected, that the major stabilizing factor is the dispersion energy. However, it should be pointed out that the MP2 method tends to overestimate this term, see *e.g.* ref. 79). Interestingly, the magnitudes of $\Delta I^{(20)}_{\text{disp}}$ are notably smaller compared to the first-order terms, especially for the modes ν_{56} and ν_{57}, localized on 1,3,5-trifluorobenzene. Even in the case of mode ν_{24} localized on benzene, for which the delocalization plays only a minor role, the absolute value of $\Delta I^{(20)}_{\text{disp}}$ is roughly three times smaller than the first-

Table 2 Excess IR intensity (ΔI, see eqn (10)) and interaction energy (ΔE, see eqn (12)–(14)) decomposition in the B···T complex

	$X = E$ (kcal mol^{-1})		$X = I$ (km mol^{-1})				
	B···T	HCN···HNC	B···T			HCN···HNC	
Term			ν_{24}	ν_{56}	ν_{57}	ν_3	ν_{12}
$\Delta X^{(10)}_{\text{el}}$	−8.77	−10.22	29.92	−28.47	−55.94	7.43	61.35
$\Delta X^{\text{HL}}_{\text{ex}}$	19.57	9.37	−24.99	−58.98	−17.29	−10.58	−8.76
$\Delta X^{\text{HF}}_{\text{del}}$	−2.08	−4.19	−2.89	61.02	34.58	8.85	30.68
$\Delta X^{\text{HF}}_{\text{int}}$	8.72	−5.04	2.04	−26.44	−38.65	5.70	83.27
$\Delta X^{(12)}_{\text{el,r}}$	0.19	−0.52	−3.91	7.12	7.12	−0.33[a]	4.38[b]
$\Delta X^{(2)}_{\text{ex}}$	3.50	1.41	−0.34	−9.15	−2.03	−0.33[a]	4.38[b]
$\Delta X^{(20)}_{\text{disp}}$	−17.85	−3.41	11.05	4.07	−3.05	0.50	0.00
$\Delta X^{\text{MP2}}_{\text{int}}$	−5.44	−7.56	8.84	−24.41	−36.61	5.54	92.03

[a] The difference in both contributions is approximately 4×10^{-3} km mol^{-1}. [b] The difference in both contributions is smaller than 10^{-3} km mol^{-1}.

order electrostatic contribution ($\Delta I^{(10)}_{\text{el}}$). By and large, except for mode ν_{24}, the sum of first-order terms contributing to the interaction-induced IR intensity ($\Delta I^{(10)}_{\text{el}} + \Delta I^{\text{HL}}_{\text{ex}}$), as well as $\Delta I^{\text{HF}}_{\text{int}}$, prevail over the dispersion contribution ($\Delta I^{(20)}_{\text{disp}}$). This is in contrast with the interplay of components observed for the interaction energy. Consequently, for the two modes localized on 1,3,5-trifluorobenzene the intensity changes can be reliably predicted at the HF level, as higher-order interaction terms are small and

cancel each other out. In the case of these two modes the qualitative pattern is similar, *i.e.* electrostatic and exchange interactions quench the IR intensity, while the delocalization term (encompassing induction contributions) has the opposite effect. On the other hand, the increase in the intensity of the mode ν_{24} upon the formation of the complex is mainly due to the interplay of large opposite-sign first-order components (positive electrostatic and negative exchange) and smaller dispersion contribution.

We will now turn to the analysis of data obtained for the HCN···HNC complex. We chose two normal modes for the analysis, *i.e.* a non-localized intermolecular N–H stretching mode formed due to hydrogen bonding (ν_4 in the complex, 174 cm^{-1}) and the C–H stretching mode localized on HCN (ν_{12} in the complex, 3447 cm^{-1}). The corresponding data are presented in Tables 1 and 2. The pattern of interaction types governing stability is typical for hydrogen-bonded complexes,[57,80,81] *i.e.* there is a large electrostatic component (quenched to a large extent by associated first-order exchange) and a smaller, but still significant stabilizing contribution from the delocalization term. Taken together, these components lead to a stabilizing interaction energy at the Hartree–Fock level. Higher-order corrections further contribute to the stabilization of the HCN···HNC complex. The analysis of interaction-induced IR intensity changes reveals that the qualitative pattern for ν_4 and ν_{12} is similar, *i.e.* ΔI changes are governed by first-order electrostatic and exchange components and the delocalization term while the higher-order terms are much smaller; moreover, the signs of individual terms contributing to $\Delta I_{\mathrm{int}}^{\mathrm{HF}}$ follow the same trend – only the exchange component diminishes the intensity. Note that such a pattern was not found in the case of the investigated modes of the B···T complex. Even though we analyzed two different stretching vibrations in the linear hydrogen-bonded system (intra- and inter-molecular stretching) and the magnitudes of ΔI remain very different, the overall pattern of the dominant components remains similar.

Finally, let us comment on the differences between ΔI shown in Tables 1 and 2. The intensity changes presented in Table 1 include the effect of monomer relaxation, *i.e.*:

$$\Delta I_a = I_a(\mathbf{AB_{AB}}) - I_a(\mathbf{A_A}) - I_a(\mathbf{B_B})$$

where $\mathbf{AB_{AB}}$, $\mathbf{A_A}$ and $\mathbf{B_B}$ correspond to dimer and both monomers at their relaxed geometries (indicated by subscripts), respectively. For a vibrational mode a localized, *e.g.*, on monomer **A**, the intensity change can be expressed as follows:

$$\Delta I_a = I_a(\mathbf{AB_{AB}}) - I_a(\mathbf{A_A})$$

Since the proposed decomposition scheme for ΔI is based on the definition of interaction energy, the corresponding formula for ΔI reads

$$\Delta I_a = I_a(\mathbf{AB_{AB}}) - I_a(\mathbf{A_{AB}}) - I_a(\mathbf{B_{AB}})$$

Hence, the differences in ΔI between the two tables can be directly related to the effect of geometry deformation upon complex formation and its influence on the IR intensity changes. For the studied modes of the B···T complex this effect is negligible for mode ν_{24}, and one-order of magnitude smaller than the major contribution for ν_{56} and ν_{57}. These findings are in agreement with the results obtained for two modes corresponding to the hydrogen-bonded complex where the effect of monomer relaxation does not exceed 8% of the total ΔI value.

5. Summary and outlook

In summary, we have presented a new decomposition scheme for interpreting the IR intensity changes on passing from isolated subsystems to molecular complexes in terms of interaction types. To illustrate its potential we have applied the newly developed scheme to two important classes of molecular complexes: hydrogen-bonded (HCN···HNC) and π···π stacked (benzene···1,3,5-trifluorobenzene) systems. In more detail, we have analyzed three intense vibrational modes in the benzene···1,3,5-trifluorobenzene complex, namely the in-phase out-of-plane C–H bending of benzene and the C–C symmetric and asymmetric stretching modes of 1,3,5-trifluorobenzene. In the case of the HCN···HNC complex we analyzed two modes: the C–H stretching mode localized on HCN and a low-frequency non-localized mode appearing due to intermolecular interaction. We have thus demonstrated that the method can be employed to decompose the IR intensity changes upon complex formation for modes localized on monomers as well as non-localized modes appearing due to intermolecular interactions. The exemplary applications revealed that the interplay of interaction energy components governing stability (ΔE_{int}) might qualitatively differ from that corresponding to IR intensity changes (ΔI), *e.g.*, in the case of the dispersion-bound π···π-stacking complex, the dispersion contributions to the interaction induced IR intensity of the selected modes are notably smaller than the magnitudes of first-order (electrostatic and exchange) terms. The new scheme can also be applied to other types of neutral and charged complexes (halogen-bonded, tetrel-bonded, inclusive, atom-molecule, *etc.*).[82–85] Provided that the shift of vibrational frequency upon complex formation is negligible, the proposed scheme allows the direct decomposition of infrared intensity changes; otherwise the change of intensity/frequency ratio can be decomposed providing useful information about the contribution of different interaction types to the net changes in IR spectroscopic signatures. The decomposition of IR intensity changes was realised *via* the variational–perturbational energy decomposition scheme at the MP2 level, but it can also be performed in combination with other EDA approaches. The proposed scheme thus represents a general tool that provides new physical insights into the manifestation of intermolecular forces in spectral properties of molecular complexes.

Conflicts of interest

There are no conflicts to declare.

Acknowledgements

R. Z. gratefully acknowledges support from the National Science Centre, Poland (Grant 2018/30/E/ST4/00457). J. M. L.

is thankful for the funds from the Spanish government MICINN (PGC2018-098212-B-C22), and the Generalitat de Catalunya (2021SGR00623). The authors thank the Wroclaw Centre for Networking and Supercomputing for the generous allotment of computer time. The authors thank Miss Elizaveta F. Petrusevich for the preparation of the graphical abstract.

Notes and references

1 G. R. Desiraju, *J. Am. Chem. Soc.*, 2013, **135**, 9952–9967.
2 P. A. Gale, J. T. Davis and R. Quesada, *Chem. Soc. Rev.*, 2017, **46**, 2497–2519.
3 A. Buckingham, J. Del Bene and S. McDowell, *Chem. Phys. Lett.*, 2008, **463**, 1–10.
4 T. Fornaro, D. Burini, M. Biczysko and V. Barone, *J. Phys. Chem. A*, 2015, **119**, 4224–4236.
5 B. Jeziorski, R. Moszyński and K. Szalewicz, *Chem. Rev.*, 1994, **94**, 1887–1930.
6 K. Morokuma, *J. Chem. Phys.*, 1971, **55**, 1236–1244.
7 T. Ziegler and A. Rauk, *Theoret. Chim. Acta*, 1977, **46**, 1–10.
8 K. Kitaura and K. Morokuma, *Int. J. Quantum Chem.*, 1976, **10**, 325–340.
9 P. S. Bagus, K. Hermann and C. W. Bauschlicher, *J. Chem. Phys.*, 1984, **80**, 4378.
10 W. J. Stevens and W. H. Fink, *Chem. Phys. Lett.*, 1987, **139**, 15–22.
11 E. D. Glendening and A. Streitwieser, *J. Chem. Phys.*, 1994, **100**, 2900.
12 Y. Mo, J. Gao and S. D. Peyerimhoff, *J. Chem. Phys.*, 2000, **112**, 5530.
13 P. Su and H. Li, *J. Chem. Phys.*, 2009, **131**, 014102.
14 P. R. Horn and M. Head-Gordon, *Phys. Chem. Chem. Phys.*, 2016, **18**, 23067.
15 K. Müller-Dethlefs and P. Hobza, *Chem. Rev.*, 2000, **100**, 143–167.
16 J. P. Wagner and P. R. Schreiner, *Angew. Chem., Int. Ed.*, 2015, **54**, 12274–12296.
17 P. Fowler and A. Sadlej, *Mol. Phys.*, 1992, **77**, 709–725.
18 D. M. Bishop and M. Dupuis, *Mol. Phys.*, 1996, **88**, 887–898.
19 T. G. A. Heijmen, R. Moszynski, P. E. S. Wormer and A. van der Avoird, *Mol. Phys.*, 1996, **89**, 81–110.
20 B. Skwara, A. Kaczmarek, R. W. Góra and W. Bartkowiak, *Chem. Phys. Lett.*, 2008, **461**, 203–206.
21 R. W. Góra, R. Zaleśny, A. Zawada, W. Bartkowiak, B. Skwara, M. G. Papadopoulos and D. L. Silva, *J. Phys. Chem. A*, 2011, **115**, 4691–4700.
22 R. W. Góra and B. Błasiak, *J. Phys. Chem. A*, 2013, **117**, 6859–6866.
23 A. Buckingham and K. Clarke, *Chem. Phys. Lett.*, 1978, **57**, 321–325.
24 P. W. Fowler, K. L. C. Hunt, H. M. Kelly and A. J. Sadlej, *J. Chem. Phys.*, 1994, **100**, 2932–2935.
25 R. Moszynski, T. G. A. Heijmen, P. E. S. Wormer and A. van der Avoird, *J. Chem. Phys.*, 1996, **104**, 6997–7007.
26 C. Hättig, H. Larsen, J. Olsen, P. Jørgensen, H. Koch, B. Fernandez and A. Rizzo, *J. Chem. Phys.*, 1999, **111**, 10099–10107.
27 H. Koch, C. Hättig, H. Larsen, J. Olsen, P. Jørgensen, B. Fernandez and A. Rizzo, *J. Chem. Phys.*, 1999, **111**, 10108–10118.
28 M. Jaszuński, A. Rizzo and P. Jørgensen, *Theor. Chem. Acc.*, 2001, **106**, 251–258.
29 A. Rizzo, C. Hättig, B. Fernandez and H. Koch, *J. Chem. Phys.*, 2002, **117**, 2609–2618.
30 J. L. Cacheiro, B. Fernandez, D. Marchesan, S. Coriani, C. Hättig and A. Rizzo, *Mol. Phys.*, 2004, **102**, 101–110.
31 A. Antušek, M. Jaszuński and A. Rizzo, *J. Chem. Phys.*, 2007, **126**, 074303.
32 T. Bancewicz and G. Maroulis, *Chem. Phys. Lett.*, 2010, **498**, 349–352.
33 A. Chantzis and G. Maroulis, *Chem. Phys. Lett.*, 2011, **507**, 42–47.
34 D. Xenides, A. Hantzis and G. Maroulis, *Chem. Phys.*, 2011, **382**, 80–87.
35 G. Maroulis, A. Haskopoulos, W. Glaz, T. Bancewicz and J. Godet, *Chem. Phys. Lett.*, 2006, **428**, 28–33.
36 B.-Q. Wang, Z.-R. Li, D. Wu, X.-Y. Hao, R.-J. Li and C.-C. Sun, *J. Phys. Chem. A*, 2004, **108**, 2464–2468.
37 B. Skwara, W. Bartkowiak, A. Zawada, R. W. Góra and J. Leszczynski, *Chem. Phys. Lett.*, 2007, **436**, 116–123.
38 A. Baranowska, B. Fernandez, A. Rizzo and B. Jansik, *Phys. Chem. Chem. Phys.*, 2009, **11**, 9871–9883.
39 A. Baranowska, A. Zawada, B. Fernandez, W. Bartkowiak, D. Kedziera and A. Kaczmarek-Kedziera, *Phys. Chem. Chem. Phys.*, 2010, **12**, 852–862.
40 A. Baranowska, B. Fernandez and A. J. Sadlej, *Theor. Chem. Acc.*, 2011, **128**, 555–561.
41 A. Zawada, R. W. Góra, M. M. Mikołajczyk and W. Bartkowiak, *J. Phys. Chem. A*, 2012, **116**, 4409–4416.
42 A. Zawada, A. Kaczmarek-Kedziera and W. Bartkowiak, *J. Mol. Model.*, 2012, **18**, 3073–3086.
43 M. H. Champagne, X. Li and K. L. C. Hunt, *J. Chem. Phys.*, 2000, **112**, 1893–1906.
44 X. Li, C. Ahuja, J. F. Harrison and K. L. C. Hunt, *J. Chem. Phys.*, 2007, **126**, 214302.
45 T. Karman, E. Miliordos, K. L. C. Hunt, G. C. Groenenboom and A. van der Avoird, *J. Chem. Phys.*, 2015, **142**, 084306.
46 M. Abel, L. Frommhold, X. Li and K. L. C. Hunt, *J. Phys. Chem. A*, 2011, **115**, 6805–6812.
47 M. Abel, L. Frommhold, X. Li and K. L. C. Hunt, *J. Chem. Phys.*, 2012, **136**, 044319.
48 C. D. Zeinalipour-Yazdi and D. P. Pullman, *J. Phys. Chem. B*, 2006, **110**, 24260–24265.
49 G. Maroulis, *Int. J. Quant. Chem.*, 2012, **112**, 2231–2241.
50 J.-L. Godet, T. Bancewicz, W. Glaz, G. Maroulis and A. Haskopoulos, *J. Chem. Phys.*, 2009, **131**, 204305.
51 A. Baranowska-Łaczkowska, B. Fernandez, A. Rizzo and B. Jansik, *Mol. Phys.*, 2012, **110**, 2503–2512.
52 Ż. Czyżnikowska, R. W. Góra, R. Zaleśny, W. Bartkowiak, A. Baranowska-Łaczkowska and J. Leszczynski, *Chem. Phys. Lett.*, 2013, **555**, 230–234.
53 A. Baranowska-Łaczkowska, B. Fernandez and R. Zaleśny, *J. Comp. Chem.*, 2013, **34**, 275–283.

54 A. Baranowska-Łaczkowska and B. Fernandez, *Mol. Phys.*, 2015, **113**, 3362–3369.
55 M. Medved, Š. Budzak, A. D. Laurent and D. Jacquemin, *J. Phys. Chem. A*, 2015, **119**, 3112–3124.
56 R. Zaleśny, M. Garcia-Borrás, R. Góra, M. Medved and J. M. Luis, *Phys. Chem. Chem. Phys.*, 2016, **18**, 22467–22477.
57 R. Zaleśny, M. Medved, R. W. Góra, H. Reis and J. M. Luis, *Phys. Chem. Chem. Phys.*, 2018, **20**, 19841–19849.
58 M. Medved, A. Iglesias, H. Reis, R. Gora, J. M. Luis and R. Zaleśny, *Phys. Chem. Chem. Phys.*, 2020, **22**, 4225–4234.
59 D. Bishop, *Adv. Chem. Phys.*, 1998, **104**, 1–40.
60 D. Bishop and B. Kirtman, *J. Chem. Phys.*, 1991, **95**, 2646–2658.
61 D. M. Bishop and B. Kirtman, *J. Chem. Phys.*, 1992, **97**, 5255–5256.
62 D. M. Bishop, J. M. Luis and B. Kirtman, *J. Chem. Phys.*, 1998, **108**, 10008–10012.
63 D. M. Bishop, M. Hasan and B. Kirtman, *J. Chem. Phys.*, 1995, **103**, 4157–4159.
64 C. Eckart, *Phys. Rev.*, 1926, **28**, 711.
65 J. M. Luis, M. Duran, J. L. Andrés, B. Champagne and B. Kirtman, *J. Chem. Phys.*, 1999, **111**, 875.
66 M. Gutowski, F. V. Duijneveldt, G. Chałasińńśki and L. Piela, *Mol. Phys.*, 1987, **61**, 233–247.
67 W. A. Sokalski, S. Roszak and K. Pecul, *Chem. Phys. Lett.*, 1988, **153**, 153–159.
68 S. M. Cybulski, G. Chałasiński and R. Moszyński, *J. Chem. Phys.*, 1990, **92**, 4357–4363.
69 G. Chałasiński and M. M. Szcześniak, *Chem. Rev.*, 1994, **94**, 1723–1765.
70 G. Chałasiński and M. M. Szcześniak, *Mol. Phys.*, 1988, **63**, 205–224.
71 F. B. van Duijneveldt, J. G. C. M. van Duijneveldt-van de Rijdt and J. H. van Lenthe, *Chem. Rev.*, 1994, **94**, 1873–1885.
72 R. Moszyński, S. Rybak, S. Cybulski and G. Chałasiński, *Chem. Phys. Lett.*, 1990, **166**, 609–614.
73 T. H. Dunning, *J. Chem. Phys.*, 1989, **90**, 1007–1023.
74 R. A. Kendall, T. H. Dunning and R. J. Harrison, *J. Chem. Phys.*, 1992, **96**, 6796–6806.
75 D. E. Woon and T. H. Dunning, *J. Chem. Phys.*, 1994, **100**, 2975–2988.
76 M. J. Frisch, G. W. Trucks, H. B. Schlegel, G. E. Scuseria, M. A. Robb, J. R. Cheeseman, G. Scalmani, V. Barone, B. Mennucci, G. A. Petersson, H. Nakatsuji, M. Caricato, X. Li, H. P. Hratchian, A. F. Izmaylov, J. Bloino, G. Zheng, J. L. Sonnenberg, M. Hada, M. Ehara, K. Toyota, R. Fukuda, J. Hasegawa, M. Ishida, T. Nakajima, Y. Honda, O. Kitao, H. Nakai, T. Vreven, J. A. Montgomery, Jr., J. E. Peralta, F. Ogliaro, M. Bearpark, J. J. Heyd, E. Brothers, K. N. Kudin, V. N. Staroverov, R. Kobayashi, J. Normand, K. Raghavachari, A. Rendell, J. C. Burant, S. S. Iyengar, J. Tomasi, M. Cossi, N. Rega, J. M. Millam, M. Klene, J. E. Knox, J. B. Cross, V. Bakken, C. Adamo, J. Jaramillo, R. Gomperts, R. E. Stratmann, O. Yazyev, A. J. Austin, R. Cammi, C. Pomelli, J. W. Ochterski, R. L. Martin, K. Morokuma, V. G. Zakrzewski, G. A. Voth, P. Salvador, J. J. Dannenberg, S. Dapprich, A. D. Daniels, O. Farkas, J. B. Foresman, J. V. Ortiz, J. Cioslowski and D. J. Fox, *Gaussian 09 Revision D.01*, Gaussian Inc., Wallingford CT, 2009.
77 M. W. Schmidt, K. K. Baldridge, J. A. Boatz, S. T. Elbert, M. S. Gordon, J. H. Jensen, S. Koseki, N. Matsunaga, K. A. Nguyen, S. Su, T. L. Windus, M. Dupuis and J. A. Montgomery, *J. Comput. Chem.*, 1993, **14**, 1347–1363.
78 R. W. Gora, *EDS package, Revision 2.8.3*, Wrocław, Poland, 1998–2008.
79 S. M. Cybulski and M. L. Lytle, *J. Chem. Phys.*, 2007, **127**, 141102.
80 Ż. Czyżnikowska, P. Lipkowski, R. W. Góra, R. Zaleśny and A. C. Cheng, *J. Phys. Chem. B*, 2009, **113**, 11511–11520.
81 Z. Czyżnikowska, R. W. Góra, R. Zaleśny, P. Lipkowski, K. N. Jarzembska, P. M. Dominiak and J. Leszczynski, *J. Phys. Chem. B*, 2010, **114**, 9629–9644.
82 J. T. Kelly, T. L. Ellington, T. M. Sexton, R. C. Fortenberry, G. S. Tschumper and K. R. Asmis, *J. Chem. Phys.*, 2018, **149**, 191101.
83 G. Cavallo, P. Metrangolo, R. Milani, T. Pilati, A. Priimagi, G. Resnati and G. Terraneo, *Chem. Rev.*, 2016, **116**, 2478–2601.
84 S. Scheiner, *Phys. Chem. Chem. Phys.*, 2021, **23**, 5702–5717.
85 A. A. Popov, S. Yang and L. Dunsch, *Chem. Rev.*, 2013, **113**, 5989–6113.

